Scientific Research Publishing

Optics and Photonics Journal, 2020, 10, 251-263
https://www.scirp.org/journal/opj
ISSN Online: 2160-889X
ISSN Print: 2160-8881

Passively Q-Switched Erbium-Doped Fiber Laser with $TiSe_2$ as Saturable Absorber

Zhifeng Hong, Ying Liu, Fuhao Yang, Xiaojuan Liu*, Huanian Zhang, Liping Guo, Xiaolu Ge

School of Physics and Optoelectronic Engineering, Shandong University of Technology, Zibo, China
Email: *liuxiaojuansd@163.com

How to cite this paper: Hong, Z.F., Liu, Y., Yang, F.H., Liu, X.J., Zhang, H.N., Guo, L.P. and Ge, X.L. (2020) Passively Q-Switched Erbium-Doped Fiber Laser with $TiSe_2$ as Saturable Absorber. *Optics and Photonics Journal*, **10**, 251-263.
https://doi.org/10.4236/opj.2020.1011024

Received: November 11, 2020
Accepted: November 27, 2020
Published: November 30, 2020

Abstract

The $TiSe_2$ nanosheets were prepared by means of ultrasound-assisted liquid phase exfoliation (LPE) and the nonlinear saturable absorption properties were experimentally investigated. The modulation depth, saturation intensity and nonsaturable absorbance of the prepared 1T-$TiSe_2$ SA were 15.7%, 1.28 MW/cm^2 and 8.2%, respectively. Taking advantage of the saturable absorption properties of $TiSe_2$-based SA, a passively Q-switched erbium-doped fiber (EDF) laser was systematically demonstrated. The pulse repetition rates varied from 24.50 kHz up to 73.79 kHz with the increasing pump power. The obtained shortest pulse width was 1.31 μs with pulse energy of 79.28 nJ. The system presented merits of low-cost SA preparation, system compactness, superb stability and high competition.

Keywords

Q-Switched Fiber Laser, 1T-Phase Titanium Diselenide (1T-$TiSe_2$), Saturable Absorber (SA), Erbium-Doped Fiber (EDF), Two-Dimensional (2D) Materials

1. Introduction

Compared to continuous-wave (CW) lasers, short-pulse lasers can remarkably improve some applications due to the much higher peak power with much lower average power lever. Passively Q-switching and mode-locking using saturable absorbers (SAs) are the main mechanisms to modulate the laser operation from CW into pulsed regime, and SAs play a vital role in such processes [1] [2] [3].

In the race towards new SAs, researchers have paid increasing attention to pursuing materials with features of wider saturable absorption bands, higher nonlinearity, larger modulation depth and higher carrier mobility. Among them, two-dimensional (2D) materials have been fully investigated in optics operations as SAs from 2004 [4]-[10]. Every kind of 2D materials presents both unique ad-

vantages and specific disadvantages [11] [12]. Especially transition metal dichalcogenides (TMDs), a family of 2D materials, are characterized by naturally large band gaps that they are unavailable for the mid-infrared region (MIR). Although they can be reduced to the level available for mid-infrared application by introducing a series of defects, the preparation process and cost are complicated.

However, the idea has been renewed by the appearance of 1T-phase titanium diselenide (1T-$TiSe_2$), a model 2D transition metal dichalcogenide (TMDs), because of the semimetal behavior with overlapping valence and conduction bands. Firstly, its bandgap is as narrow as 0.15 electon-volt (eV), even smaller or non-existent [13], which, compared with other members of TMDs, is more advantageous in supporting broadband response from the visible to MIR wave band. Secondly, the layered crystalline structure of 1T-$TiSe_2$ has relatively weaker van der Waals forces between interlayers than most TMDs, which makes it easier to exfoliate films with different thickness from bulk form. Furthermore, it is characterized by ultrafast relaxation time (in the sub-100-fs range), large number of carriers, and strong light–matter interactions. The merits above make 1T-$TiSe_2$ a promising broadband SA for passively Q-switched and mode-locked lasers.

In 2013, 1T-$TiSe_2$ was firstly applied in passively Q-switched solid-state lasers by Bingzheng Yan *et al.* [13]. The shortest pulse widths were 483, 344, 350, and 160 ns with the highest repetition rates of 152, 224, 84, and 78 kHz at lasing wavelength of 1.0, 1.3, 2.0, and 2.8 μm, respectively. In 2018, a passively Q-switched laser operating at 2.95 μm based on an 1T-$TiSe_2$ SA was first realized by Hongkun Nie *et al.* [14], where a pulse width as short as 160.5 ns was generated at a repetition rate of 98.9 kHz. 1T-$TiSe_2$ has as well been applied in passively Q-switched fiber lasers. In 2018, Wenjun Liu *et al.* firstly achieved a passively Q-switched erbium-doped fiber (EDF) laser operating at 1530 nm based on 1T-$TiSe_2$ SA mirror (SAM) [15], hence a fraction of free space optical-path is involved. The shortest pulse duration was 1.126 μs with the corresponding repetition rate and output power of 154 kHz and 11.54 milliwatt (mW), respectively. On aspect of preparation of the 1T-$TiSe_2$ SA, the method is more costly and complex than the 1T-$TiSe_2$ SA utilized both in our paper and previously reported papers.

In this contribution, we demonstrate a passively Q-switched EDF laser operating at 1560.472 nanometer (nm) with simple ring cavity configuration based on 1T-$TiSe_2$ SA. The pulse repetition rates vary from 24.50 kHz up to 73.79 kHz with the increasing pump power. The obtained shortest pulse width and pulse energy are 1.31 microsecond (μs) and 79.28 nanojoule (nJ), respectively. Comparatively, the work is characterized by merits of simple as well as low-cost SA preparation process, compactness, superb stability and high competition. On the other hand, the system is free of air-space, which means a total-fiber system with advantages of integrated structure and convenient maintenance in practical applications.

2. Preparation and Characterization of 1T-$TiSe_2$ SA

In this work, ultrasound-assisted liquid phase exfoliation (LPE), an easy and low-cost method is adopted to prepare the 1T-$TiSe_2$ nanosheets. Firstly, 10 mg 1T-$TiSe_2$ powder is dispersed into 10 milliliter (ml) 30% alcohol. The mixture is stirred for 30 minutes and subsequently, undergoes ultrasonication for 3 hours to obtain 1T-$TiSe_2$ dispersion. Then the dispersion solution is further centrifuged at a rate of 1500 revolutions per minute (rpm) for 30 minutes until the 1T-$TiSe_2$ is thoroughly dispersed and supernatant liquor is collected for the subsequent experiments, which is shown in **Figure 1**. After that, 160 milligram (mg) polyvinyl acetate (PVA) is added into 4 ml 1T-$TiSe_2$ dispersion, and the mixture undergoes 2 hours ultrasonication process to prepare uniform 1T-$TiSe_2$-PVA dispersion. PVA is used as the polymer matrix both to form film to host the 1T-$TiSe_2$ and to avoid its oxidation. A single drop of the obtained 1T-$TiSe_2$ solution is immersed on the end of the fiber. Then, the sample is dried for 24 hours at a temperature of 25˚C and finally, the 1T-$TiSe_2$ SA is obtained.

As shown in **Figure 2(a)** and **Figure 2(b)**, the surface morphology of 1T-$TiSe_2$ is analyzed by using scanning electron microscopy (SEM) and transmission electron microscopy (TEM), where the clear appearance and uniform lattice fringes of 1T-$TiSe_2$ are presented. **Figure 2(c)** shows the higher resolution TEM (HRTEM) image, which exhibits no obvious defect. The selected area electron diffraction (SAED) image shown in **Figure 2(d)**, depicts a high crystallinity.

The Raman spectrum of 1T-$TiSe_2$ nanosheets is tested and shown in **Figure 3**. The in-plane mode (E_g) and out-of-plane mode (A_{1g}) can be clearly observed. The E_g peak is located at 134.15 cm^{-1} while A_{1g} peak at 198.04 cm^{-1}, which matches closely with the previous reports [13].

To confirm the thickness of the prepared 1T-$TiSe_2$-SA, an atomic force microscopy (AFM) is implemented. The AFM image and height profiles are shown in **Figure 4(a)** and **Figure 4(b)**. The thickness of the transferred layers in the investigated area is found to be ~16 nm, corresponding to the layer number of ~28 [14].

Figure 1. Supernatant liquor of the 1T-$TiSe_2$ nanosheets.

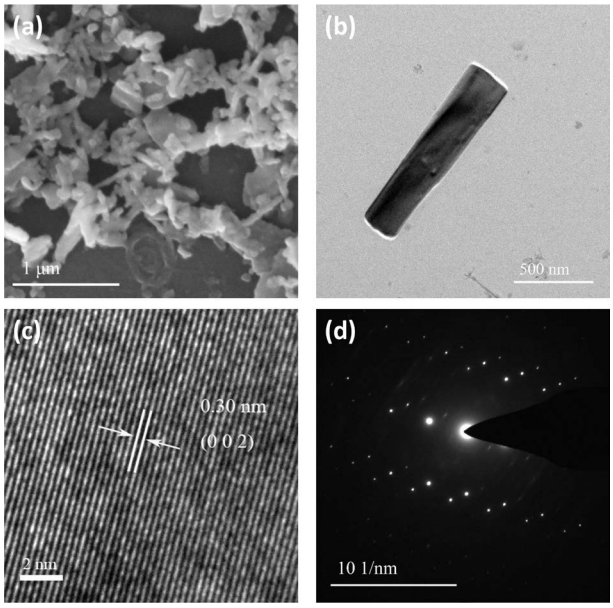

Figure 2. (a) SEM image of 1T-$TiSe_2$ nanosheets. (b) TEM image of 1T-$TiSe_2$ nanosheets. (c) The high resolution image of 1T-$TiSe_2$ nanosheets. (d) The selected area electron diffraction of 1T-$TiSe_2$ nanosheets.

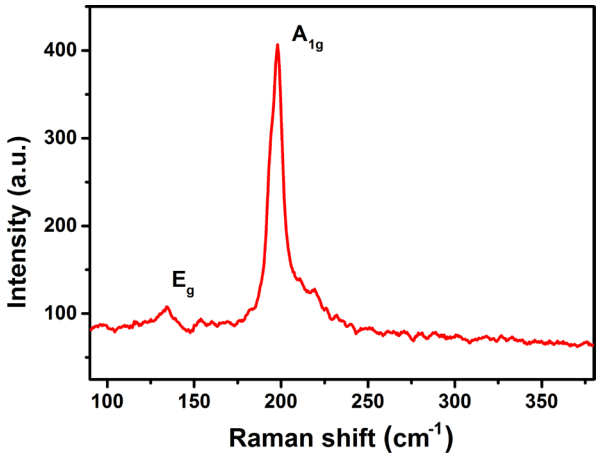

Figure 3. Raman spectrum of the prepared 1T-$TiSe_2$ nanosheets.

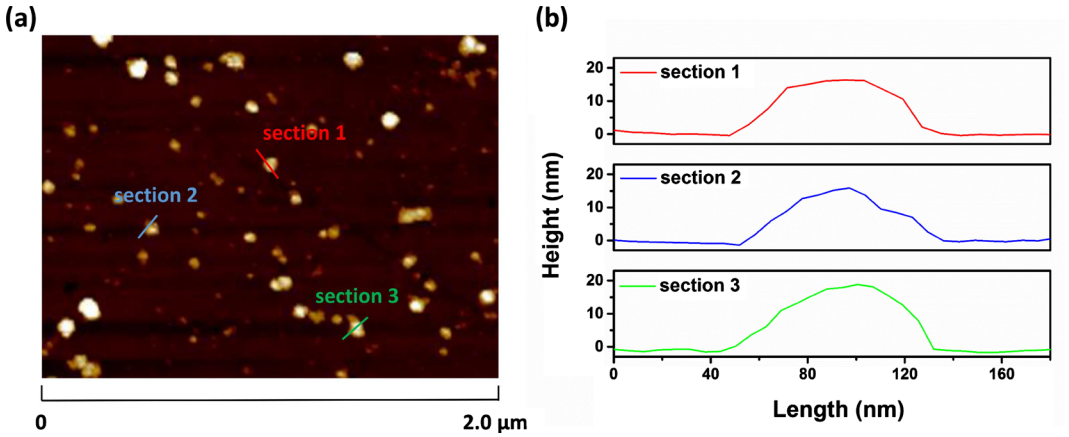

Figure 4. The AFM of the 1T-$TiSe_2$ nanosheets.

The nonlinear optical absorption properties of the 1T-$TiSe_2$—based SA are investigated by the commonly-used balanced twin-detector measurement scheme. A fiber laser operating at central wavelength of 1550 nm is utilized with 10 ps pulse duration and fundamental frequency of 13.1 MHz, respectively. The nonlinear power-dependent normalized saturable absorption curve of the 1T-$TiSe_2$ SA is presented as blue dots in Figure 5. It is seen that as the light intensity gradually increases, the nonlinear optical transmission approximately increases to 91.8% and remains saturated there, which reveals a typical saturable absorption characteristic. The modulation depth, saturation intensity and nonsaturable absorbance are 15.7%, 1.28 MW/cm^2 and 8.2%, respectively. It is seen that the data matches closely to the curve, presented as red line, of the saturable absorption formula:

$$T(I) = 1 - \Delta T \times \exp(-I/I_{sat}) - T_{ns} \quad (1)$$

where $T(I)$ is transmission, ΔT is the modulation depth, I is input laser intensity, I_{sat} and T_{ns} are saturation intensity and nonsaturable absorbance, respectively [16] [17].

We also measured the linear transmission spectrum of the 1T-$TiSe_2$ nanosheets in the range of 200 - 2000 nm using a UV/VIS/NIR spectrophotometer (U-3500, Hitachi, Japan). As shown in Figure 6, the red line displays the transmittance

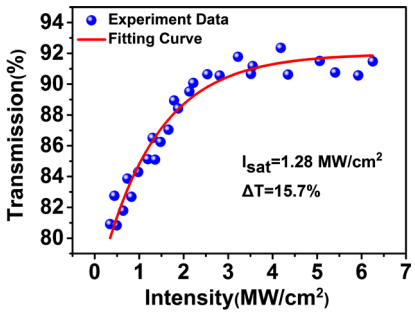

Figure 5. The nonlinear optical absorption properties of the1T-$TiSe_2$ SA.

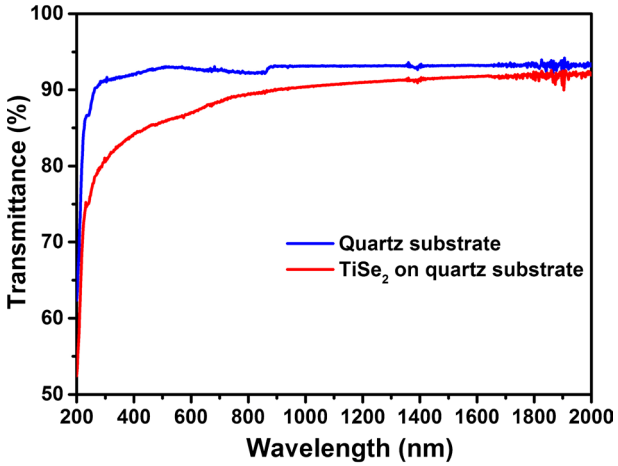

Figure 6. Linear transmission spectra of the blank quartz substrate and the 1T-$TiSe_2$ SA on quartz substrate.

of the 1T-$TiSe_2$ sheets on the quartz substrate, and the blue line displays the transmittance of the blank quartz substrate under the same conditions. In the wavelength range of 400 to 2000 nm, the transmittances of the 1T-$TiSe_2$ nanosheets and the blank quartz substrate are 90% ± 1.0% and 93% ± 0.1%, respectively meaning the net transmittance of the 1T-$TiSe_2$ nanosheets is about 97%, and the scattering loss is 3%. Besides, the result means that such a 1T-$TiSe_2$ SA enables a wider application scope.

As described in [18], a good SA should have both a high modulation depth (e.g. ~10% for fiber lasers) and a low value of saturation intensity. In the precede work [19], the modulation depth and the saturation intensity are around 6.4% and 15 gigawatts per square centimeter (GW/cm^2). While, in our work, the 1T-$TiSe_2$ SA has larger modulation depth of 15.7% and lower saturation intensity of 1.28 megawatt per square centimeter (MW/cm^2), respectively, which are much more suitable for nonlinear saturable absorption in achieving ultrafast pulses.

3. Experimental Setup

The schematic of the passively Q-switched erbium-doped fiber laser using the 1T-$TiSe_2$-based SA is given in **Figure 7**, where the laser cavity shows the ring-shaped structure. A commercial 976 nm laser diode with a maximum power of 400 mW is used as a pump, which is coupled into the laser cavity through a 980/1550 wavelength-division multiplexing (WDM). A 6 m long EDF (Nufern-EDFC-980-HP) is used as the gain medium. The prepared 1T-$TiSe_2$ SA is inserted into the cavity after the EDF. A polarization independent isolator (PI-ISO) is used to ensure the unidirectional operation of laser cavity. A polarization controller (PC) is used to optimize the cavity birefringence. Additionally, 20% of the laser power is extracted from the cavity using an optical coupler (OC). The length of the cavity, including the EDF and the tail fibers is about 11 m. The

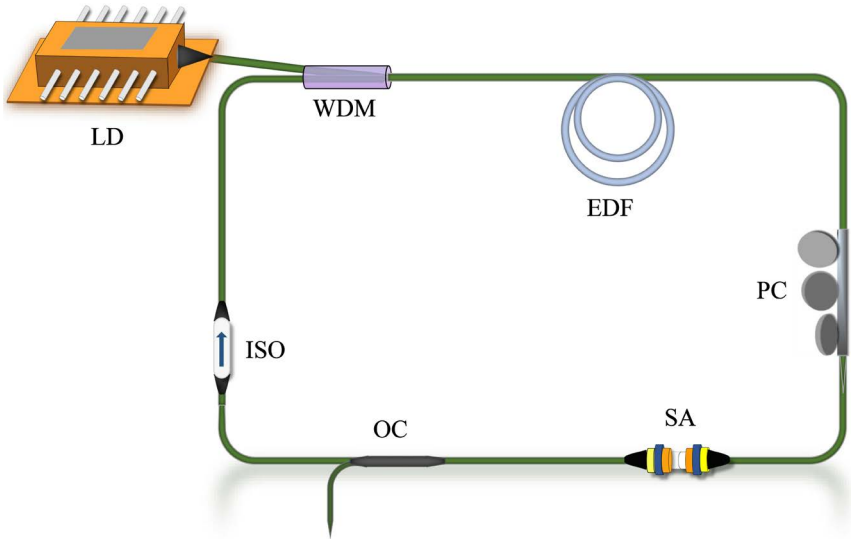

Figure 7. The schematic of the passively Q-switched EDF laser based on the 1T-$TiSe_2$ SA.

output spectrum, the pulse trace and the average output power are detected by a spectrum analyzer (YOKOGAWA AQ6370B), a digital oscilloscope (Tektronix DP04104), and a power meter (Molectron PM3), respectively.

4. Experimental Results and Discussion

At the beginning of the experiment, increase the pump power simultaneously adjust the PC to change the polarization state of the modes in the cavity. The stable passively Q-switched pulse is achieved when the pump power is increased to 37 mW. The system operates in stable Q-switched state in the 37 - 400 mW pump range.

The shortest pulse width of 1.31 μs with a repetition rate of 73.79 kHz is obtained at the pump power of 400 mW. At this moment, a single pulse envelope with the corresponding pulse sequence is recorded and separately shown in Figure 8(a) and the inset, respectively. The train of pulses is stable and there is no significant jitter on the oscilloscope. Figure 8(b) shows the output spectrum of the system, which reveals a center wavelength of 1560.472 nm.

The pulse properties in Q-switched lasers depend on nonlinear dynamics in the gain medium and SA. A pulse is emitted once a certain stored energy in the

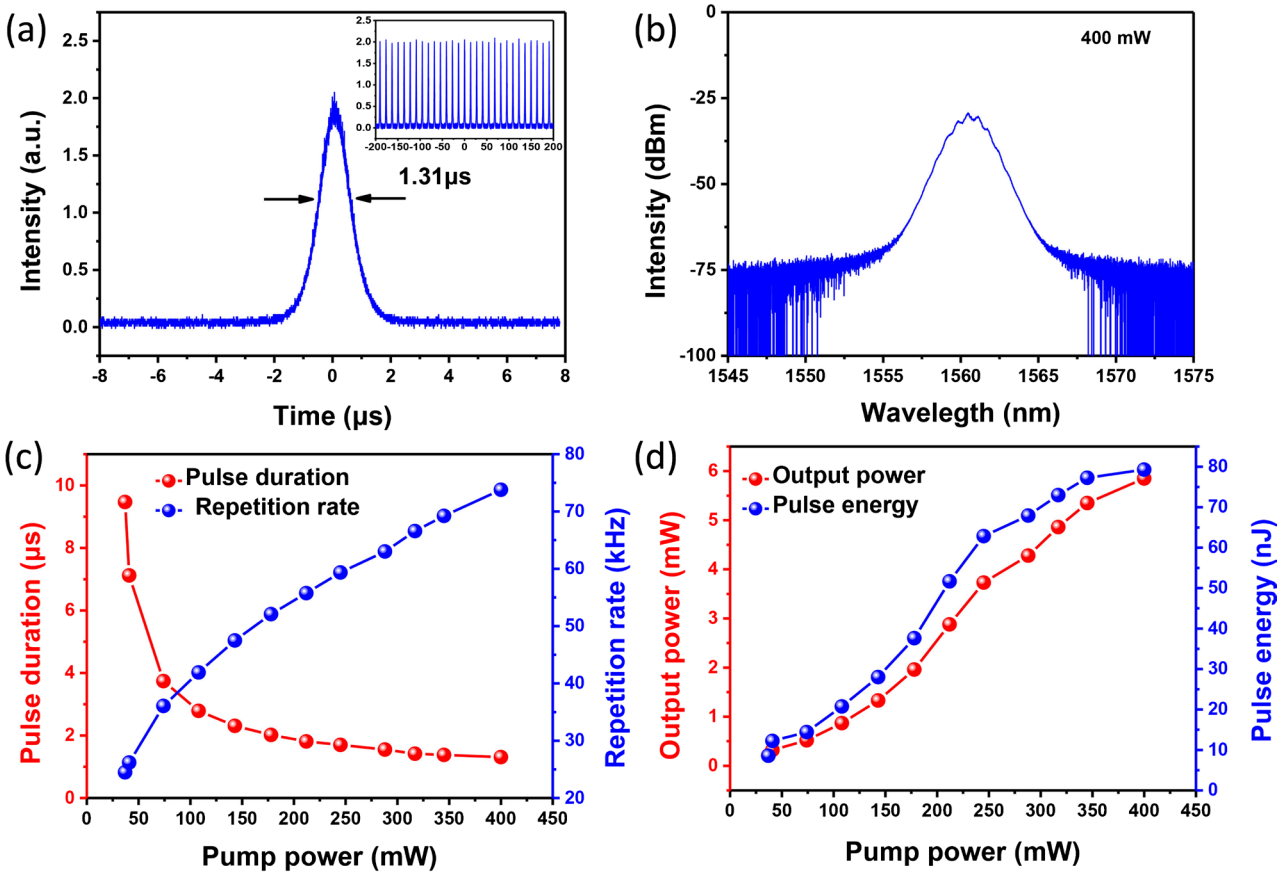

Figure 8. (a) The typical single pulse sharp of Q-switched fiber laser. The inset is the output pulse train; (b) The output spectrum of Q-switched fiber laser; (c) The pulse duration and pulse repetition rate versus the pump power; (d) The output power and pulse energy versus the pump power.

cavity is reached. This leads to a dependence of repetition rate and pulse duration upon pump power. Thus, a greater pump power enables higher repetition rates and also results in shorter pulses. This is observed experimentally and recorded in **Figure 8(c)** as the pulse duration is reduced from 9.47 μs to 1.31 μs while the repetition rate is increased from 24.50 kHz to 73.79 kHz, respectively, along with the increasing pump power from 37 to 400 mW. **Figure 8(d)** depicts the relationships of output power and the single pulse energy vs. the pump power, respectively. When the pump power is 400 mW, the obtained maximum average output power is 5.85 mW with energy of 79.28 nJ for each pulse, corresponding to optical-to-optical efficiency and slope efficiency of 1.46% and 1.55%, respectively. Although the slope efficiency is relatively low, we can further improve it by optimizing the 1T-$TiSe_2$ SA parameters and cavity design, combining with optimizing the splitting ratio of the output coupler (OC), and then increasing the pump power. Such measures have been also discussed in [20].

The pulse trains at different pump power levels are shown in **Figure 9**. During the whole experiment period for more than one month, the Q-switched pulse sequence remains highly stable. It reveals the facts that, on one hand, the 1T-$TiSe_2$ nanosheets film is free from damage at present pump power. On the other hand, the 1T-$TiSe_2$ nanosheets film presents high stability and antioxidant capacity in ambient condition, which plays a critical role in the practical applications as optical devices.

Generally, RF spectrum analyzer is employed to monitor the output pulse trains in frequency domain and better describe the noise of the Q-switched operation. However, there is no RF spectrum analyzer at present in our Lab. So alternatively [21] [22], the spectra of the Q-switched system are measured in a time duration of 2 hours with an interval of 30 min, which is shown in **Figure 10**. It can be seen that the Q-switched EDF laser exhibits an excellent stability at room temperature.

In the experiment, there is no optical damage occurred to the1T-$TiSe_2$ SA. And limited to the available pump power in our lab, the pump power limit of the

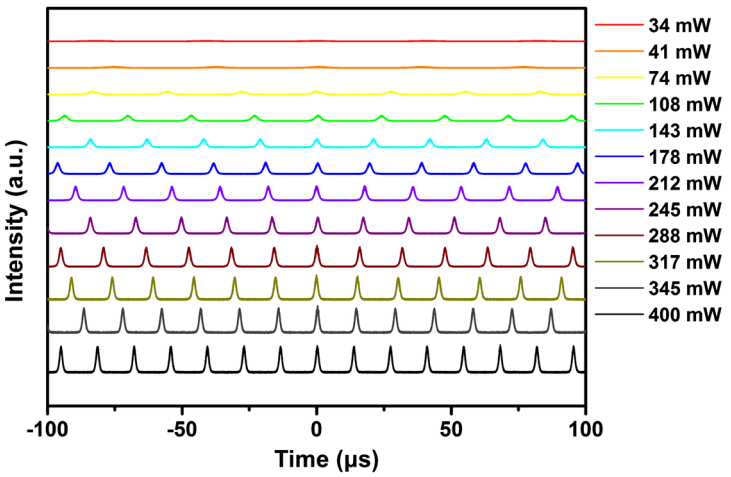

Figure 9. Pulse trains at different pump power.

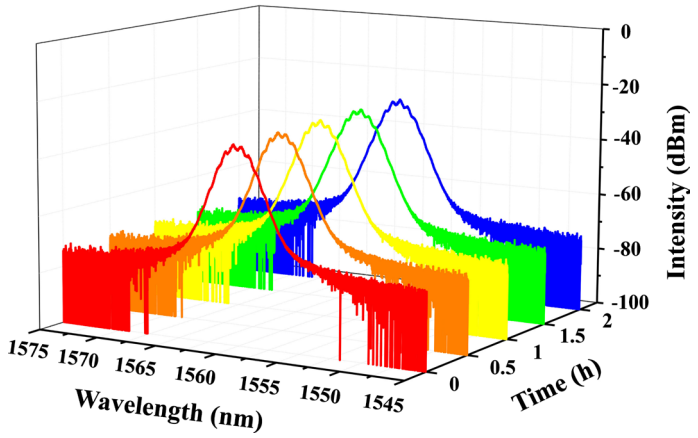

Figure 10. The measured spectra of Q-switched fiber laser at 30 min interval within a span of 2 h.

1T-$TiSe_2$ SA can not be tested.

In the first report of passively Q-switched EDF laser modulated by 1T-$TiSe_2$ SA [19], on one hand, the $TiSe_2$-SAM is prepared by a combination of magnetron sputtering method and CVD method. While, in our work, the SA is prepared by directly depositing a 1T-$TiSe_2$ nanostructured film onto the end surface of a fiber, which is much simpler, more economical as well as practical. Besides, in [19], the ring cavity is complicated, the operation is complexed and the compactness of the laser system is degraded because the existence of the free-space between the 1T-$TiSe_2$ SAM and the circular in the ring fiber laser regime. Comparatively, our total-fiber system presents a more compact construction, high stability and competitive output results with advantages of convenient maintenance and suitableness of practical applications [23].

On the other hand, as described in [18], a good SA should have both a high modulation depth (e.g. ~10% for fiber lasers) and a low value of saturation intensity. In [19], however, the modulation depth and the saturation intensity are around 6.4% and 15 GW/cm^2, respectively. The modulation depth is rather low and the saturation intensity is too high, which reveals potentiality to further compress pulses by optimizing the parameters of the 1T-$TiSe_2$ SA. While, in our work, the 1T-$TiSe_2$ SA has larger modulation depth of 15.7% and lower saturation intensity of 1.28 MW/cm^2, respectively, which are much more suitable for nonlinear saturable absorption in achieving ultrafast pulses.

Various 2D materials have been used as saturable absorbers for erbium-doped Q-switched lasers. We summarize and list the performance of current and previous EDF lasers based on various 2D saturable materials in **Table 1**. Compared with previous experimental materials, it is found that on the one hand, 1T-$TiSe_2$ nanosheets have a higher modulation depth, on the other hand, the repetition frequency, pulse duration, pulse energy and output power of the laser are highly competitive. This reveals that the 1T-$TiSe_2$ nanosheets used in this work not only have merits of low cost and simple preparation process, but also give the system characteristics of superb stability and high integration.

Table 1. Comparison of passively Q-switched EDFL performance based on different 2D materials.

Materials	Modulation Depth (%)	Repetition Rate (KHz)	Pulse durations (μs)	Pulse Energy (nJ)	Output Power (mW)	Refs
Graphene	45	3.3 - 65.9	3.7	16.7	1.1	[11]
BP	19.5	4.43 - 18	9.35	28.3	/	[24]
GNS	7.8	42.7 - 64.9	1.7	133	7.7	[25]
MoS_2	2.15	7.758 - 41.452	9.92	184.7	38.7	[26]
Bi_2Se_3	4.3	459 - 940	1.9	23.7	22.35	[4]
ZrS_2	14.7	40.65 - 87.1	1.49	33.5	2.89	[23]
SnS_2	3.15	172.3 - 233	0.51	/	9.33	[27]
$MoSe_2$	/	16.9 - 32.8	30.4	57.9	1.9	[28]
$MoWSe_2$	22	26 - 48	1.9	11.8	1.1	[29]
ZnO	3.5	41.7 - 77.2	3.0	47.9	/	[30]
WSe_2	31.25	77 - 242	1.2	110	26.7	[31]
Fe_3O_4	8.2	7.8 - 33.3	3.2	23.76	0.794	[32]
Al_2O_3	3.5	57.8 - 81	2.8	56.7	4.5	[33]
$TiSe_2$	15.7	24.5 - 73.79	1.31	79.28	5.85	Our Work

5. Conclusion

$TiSe_2$ nanosheets were prepared by means of ultrasound-assisted LPE and the nonlinear saturable absorption properties were experimentally investigated. The modulation depth, saturation intensity and nonsaturable absorbance of the prepared 1T-$TiSe_2$ SA were 15.7%, 1.28 MW/cm^2 and 8.2%, respectively. Taking advantage of the saturable absorption properties of $TiSe_2$-based SA, a passively Q-switched EDF laser was systematically demonstrated. The pulse repetition rates varied from 24.50 kHz up to 73.79 kHz with the increasing pump power. The obtained shortest pulse width was 1.31 μs with pulse energy of 79.28 nJ. Comparatively, the work is characterized by merits of simple as well as low-cost SA preparation process, compactness, superb stability and high competition. On the other hand, the system is free of air-space, which means a total-fiber system with advantages of integrated structure and convenient maintenance in practical applications.

Fund

This work is funded by the National Natural Science Funds, China (11304184), partially funded by National Natural Science Funds, China (11704226), Natural Science Foundation of Shandong Province (ZR2017MA051) and the Shandong University of Technology and Zibo City Integration Development Project (2019ZBXC120, 2018ZBXC052).

Conflicts of Interest

The authors declare no conflicts of interest regarding the publication of this paper.

References

[1] Rahman, M.F.A., Dhar, A., Das, S., Dutta, D., Paul, M.C., Rusdi, M.F.M., Latiff, A.A., Dimyati, K. and Harun, S.W. (2018) An 8cm Long Holmium-Doped Fiber Saturable Absorber for Q-Switched Fiber Laser Generation at 2-μm Region. *Optical Fiber Technology*, **43**, 67-71. https://doi.org/10.1016/j.yofte.2018.04.004

[2] Alaniz-Baylon, J., Durán-Sánchez, M., Álvarez-Tamayo, R.I., Posada-Ramírez, B., Bello-Jiménez, M., Ibarra-Escamilla, B., Castillo-Guzman, A.A. and Kuzin, E.A. (2019) Fiber Laser with Simultaneous Multi-Wavelength Er/Yb Passively Q-Switched and Single-Wavelength Tm Gain-Switched Operations. *Photonics Research*, **7**, 608-614. https://doi.org/10.1364/PRJ.7.000608

[3] Ahmad, H., Reduan, S.A. and Yusoff, N. (2018) Chitosan Capped Nickel Oxide Nanoparticles as a Saturable Absorber in a Tunable Passively Q-Switched Erbium Doped Fiber Laser. *RSC advances*, **8**, 25592-25601. https://doi.org/10.1039/C8RA04380A

[4] Yu, Z.H., Song, Y.R., Tian, J.R., Dou, Z.Y., Guoyu, H.Y., Li, K.X., Li, H.W. and Zhang, X.P. (2014) High-Repetition-Rate Q-Switched Fiber Laser with High Quality Topological Insulator Bi_2Se_3 Film. *Optics Express*, **22**, 11508-11515. https://doi.org/10.1364/OE.22.011508

[5] Ahmad, H., Aidit, S.N., Ooi, S.I. and Tiu, Z.C. (2018) Tunable Passively Q-Switched Erbium-Doped Fiber Laser with Chitosan/MoS_2 Saturable Absorber. *Optics & Laser Technology*, **103**, 199-205. https://doi.org/10.1016/j.optlastec.2018.01.032

[6] Wang, Q.H., Kalantar-Zadeh, K., Kis, A., Coleman, J.N. and Strano, M.S. (2012) Electronics and Optoelectronics of Two-Dimensional Transition Metal Dichalcogenides. *Nature Nanotechnology*, **7**, 699-712. https://doi.org/10.1038/nnano.2012.193

[7] Hu, P., Liu, F.F., Huang, Y., Liu, Y., Han, K.Z., Zhang, F. and Liu, X.J. (2019) Passively Q-Switched Ytterbium-Doped Fiber Laser Operating at 1120 nm by Molybdenum Disulfide Saturable Absorber. *Optik*, **189**, 97-102. https://doi.org/10.1016/j.ijleo.2019.05.071

[8] Li, L., Lv, R.D., Wang, J., Chen, Z.D., Wang, H.Z., Liu, S.C., Ren, W., Liu, W.J. and Wang, Y.G. (2019) Optical Nonlinearity of ZrS_2 and Applications in Fiber Laser. *Nanomaterials*, **9**, 315. https://doi.org/10.3390/nano9030315

[9] Kanazawa, T., Amemiya, T., Ishikawa, A., Upadhyaya, V., Tsuruta, K., Tanaka, T. and Miyamoto, Y. (2016) Few-Layer HfS_2 Transistors. *Scientific Reports*, **6**, Article No. 22277. https://doi.org/10.1038/srep22277

[10] Salman, A.A. and Al-Janabi, A.H. (2019) Aluminum Nanoparticles Saturable Absorber as a Passive Q-Switcher for Erbium-Doped Fiber Laser Ring Cavity Configuration. *Laser Physics*, **29**, Article ID: 045102. https://doi.org/10.1088/1555-6611/ab02f8

[11] Luo, Z.Q., Zhou, M., Weng, J., Huang, G.M., Xu, H.Y., Ye, C.C. and Cai, Z.P. (2010) Graphene-Based Passively Q-Switched Dual-Wavelength Erbium-Doped Fiber Laser. *Optics letters*, **35**, 3709-3711. https://doi.org/10.1364/OL.35.003709

[12] Liu, X.J., Hu, P., Liu, Y., Guo, L.P., Ge, X.L. and Zhang, H.N. (2020) Conventional Solitons and Bound-State Solitons in an Erbium-Doped Fiber Laser Mode-Locked by $TiSe_2$-Based Saturable Absorber. *Nanotechnology*, **31**, Article ID: 365202. https://doi.org/10.1088/1361-6528/ab8fe6

[13] Yan, B.Z., Zhang, B.T., Nie, H.K., Li, G.R., Sun, X.L., Wang, Y.R., Liu, J.T., Shi, B.N., Liu, S.D. and He, J.L. (2018) Broadband 1T-Titanium Selenide-Based Saturable Absorbers for Solid-State Bulk Lasers. *Nanoscale*, **10**, 20171-20177.

https://doi.org/10.1039/C8NR03859G

[14] Nie, H.K., Sun, X.L., Zhang, B.T., Yan, B.Z., Li, G.R., Wang, Y.R., Liu, J.T., Shi, B.N., Liu, S.D. and He, J.L. (2018) Few-Layer $TiSe_2$ as a Saturable Absorber for Nanosecond Pulse Generation in 2.95 μm Bulk Laser. *Optics Letters*, **43**, 3349-3352. https://doi.org/10.1364/OL.43.003349

[15] Liu, W.J., Liu, M.L., Lei, M., Fang, S.B. and Wei, Z.Y. (2017) Titanium Selenide Saturable Absorber Mirror for Passive Q-Switched Er-Doped Fiber Laser. *IEEE Journal of Selected Topics in Quantum Electronics*, **24**, 1-5. https://doi.org/10.1109/JSTQE.2017.2759266

[16] Yuzaile, Y.R., Awang, N.A., Zalkepali, N.U.H.H., Zakaria, Z., Latif, A.A., Azmi, A.N. and Hadi, F.A. (2019) Pulse Compression in Q-Switched Fiber Laser by Using Platinum as Saturable Absorber. *Optik*, **179**, 977-985. https://doi.org/10.1016/j.ijleo.2018.11.057

[17] Li, J., Zhao, Y., Chen, Q.Y., Niu, K.D., Sun, R.Y. and Zhang, H.N. (2017) Passively Mode-Locked Ytterbium-Doped Fiber Laser Based on SnS_2 as Saturable Absorber. *IEEE Photonics Journal*, **9**, Article No. 1506707. https://doi.org/10.1109/JPHOT.2017.2766120

[18] Fu, B., Hua, Y., Xiao, X.S., Zhu, H.W., Sun, Z.P. and Yang, C.X. (2014) Broadband Graphene Saturable Absorber for Pulsed Fiber Lasers at 1, 1.5, and 2 μm. *IEEE Journal of Selected Topics in Quantum Electronics*, **20**, 411-415. https://doi.org/10.1109/JSTQE.2014.2302361

[19] Song, Y.F., Liang, Z.M., Jiang, X.T., Chen, Y.X., Li, Z.J., Lu, L., Ge, Y.Q., Wang, K., Zheng, J.L., Lu, S.B., Ji, J.H. and Zhang, H. (2017) Few-Layer Antimonene Decorated Microfiber: Ultra-Short Pulse Generation and All-Optical Thresholding with Enhanced Long Term Stability. 2*D Materials*, **4**, Article ID: 045010. https://doi.org/10.1088/2053-1583/aa87c1

[20] Rosdin, R.Z.R.R., Ahmad, F., Ali, N.M., Harun, S.W. and Arof, H. (2014) Q-Switched Er-Doped Fiber Laser with Low Pumping Threshold Using Graphene Saturable Absorber. *Chinese Optics Letters*, **12**, 091404. https://doi.org/10.3788/COL201412.091404

[21] Rusdi, M.F.M., Rosol, A.H.A., Rahman, M.F.A., Mahyuddin, M.B.H., Latiff, A.A., Ahmad, H., Harun, S.W. and Yasin, M. (2019) Q-Switched and Mode-Locked Thulium Doped Fiber Lasers with Nickel Oxide Film Saturable Absorber. *Optics Communications*, **447**, 6-12. https://doi.org/10.1016/j.optcom.2019.04.083

[22] Kang, Z., Liu, M.Y., Li, Z.W., Li, S.Q., Jia, Z.X., Liu, C.Z., Qin, W.P. and Qin, G.S. (2018) Passively Q-Switched Erbium Doped Fiber Laser Using a Gold Nanostars Based Saturable Absorber. *Photonics Research*, **6**, 549-553. https://doi.org/10.1364/PRJ.6.000549

[23] Hu, P., Huang, Y., Liu, F.F., Liu, Y., Guo, L.P., Ge, X.L. and Liu, X.J. (2019) A Q-Switched Erbium-Doped Fiber Laser Based on ZrS_2 as a Saturable Absorber. *Chinese Optics Letters*, **17**, 080603. https://doi.org/10.3788/COL201917.080603

[24] Jiang, T., Yin, K., Zheng, X., Yu, H. and Cheng, X.A. (2015) Black Phosphorus as a New Broadband Saturable Absorber for Infrared Passively Q-Switched Fiber Lasers. https://arxiv.org/abs/1504.07341v1

[25] Fan, D.F., Mou, C.B., Bai, X.K., Wang, S.F., Chen, N. and Zeng, X.L. (2014) Passively Q-Switched Erbium-Doped Fiber Laser Using Evanescent Field Interaction with Gold-Nanosphere Based Saturable Absorber. *Optics Express*, **22**, 18537-18542. https://doi.org/10.1364/OE.22.018537

[26] Chen, B.H., Zhang, X.Y., Wu, K., Wang, H., Wang, J. and Chen, J.P. (2015). Q-

Switched Fiber Laser Based on Transition Metal Dichalcogenides MoS_2, $MoSe_2$, WS_2, and WSe_2. *Optics Express*, **23**, 26723-26737. https://doi.org/10.1364/OE.23.026723

[27] Niu, K.D., Chen, Q.Y., Sun, R.Y., Man, B.Y. and Zhang, H.N. (2017) Passively Q-Switched Erbium-Doped Fiber Laser Based on SnS_2 Saturable Absorber. *Optical Materials Express*, **7**, 3934-3943. https://doi.org/10.1364/OME.7.003934

[28] Ahmad, H., Suthaskumar, M., Tiu, Z.C., Zarei, A. and Harun, S.W. (2016) Q-Switched Erbium-Doped Fiber Laser Using $MoSe_2$ as Saturable Absorber. *Optics & Laser Technology*, **79**, 20-23. https://doi.org/10.1016/j.optlastec.2015.11.007

[29] Ahmad, H., Reduan, S.A., Aidit, S.N., Yusoff, N., Maah, M.J., Ismail, M.F. and Tiu, Z.C. (2019) Ternary $MoWSe_2$ Alloy Saturable Absorber for Passively Q-Switched Yb-, Er-and Tm-Doped Fiber Laser. *Optics Communications*, **437**, 355-362. https://doi.org/10.1016/j.optcom.2019.01.009

[30] Ahmad, H., Lee, C.S.J., Ismail, M.A., Ali, Z.A., Reduan, S.A., Ruslan, N.E., Ismail, M.F. and Harun, S.W. (2016) Zinc Oxide (ZnO) Nanoparticles as Saturable Absorber in Passively Q-Switched Fiber Laser. *Optics Communications*, **381**, 72-76. https://doi.org/10.1016/j.optcom.2016.06.073

[31] Liu, W.J., Liu, M.L., Han, H.N., Fang, S.B., Teng, H., Lei, M. and Wei, Z.Y. (2018) Nonlinear Optical Properties of WSe_2 and $MoSe_2$ Films and Their Applications in Passively Q-Switched Erbium Doped Fiber Lasers. *Photonics Research*, **6**, C15-C21. https://doi.org/10.1364/PRJ.6.000C15

[32] Bai, X.K., Mou, C.B., Xu, L.X., Wang, S.F., Pu, S.L. and Zeng, X.L. (2016) Passively Q-Switched Erbium-Doped Fiber Laser Using Fe_3O_4-Nanoparticle Saturable Absorber. *Applied Physics Express*, **9**, Article ID: 042701. https://doi.org/10.7567/APEX.9.042701

[33] Al-Hayali, S.K.M., Mohammed, D.Z., Khaleel, W.A. and Al-Janabi, A.H. (2017) Aluminum Oxide Nanoparticles as Saturable Absorber for C-Band Passively Q-Switched Fiber Laser. *Applied Optics*, **56**, 4720-4726. https://doi.org/10.1364/AO.56.004720